Functional Mesh Learning for Pattern Analysis of Cognitive Processes

Orhan Fırat*, Mete Özay*, Itır Önal*, İlke Öztekin† and Fatoş T. Yarman Vural*
*Department of Computer Engineering
Middle East Technical University, Ankara, Turkey
Email: {orhan.firat, mete.ozay, itir, vural} @ceng.metu.edu.tr
†Department of Psychology
Koç University, Istanbul, Turkey
Email: ioztekin@ku.edu.tr

***Abstract*—We propose a statistical learning model for classifying cognitive processes based on distributed patterns of neural activation in the brain, acquired via functional magnetic resonance imaging (fMRI). In the proposed learning machine, local meshes are formed around each voxel. The distance between voxels in the mesh is determined by using functional neighborhood concept. In order to define functional neighborhood, the similarities between the time series recorded for voxels are measured and functional connectivity matrices are constructed. Then, the local mesh for each voxel is formed by including the functionally closest neighboring voxels in the mesh. The relationship between the voxels within a mesh is estimated by using a linear regression model. These relationship vectors, called Functional Connectivity aware Local Relational Features (FC-LRF) are then used to train a statistical learning machine. The proposed method was tested on a recognition memory experiment, including data pertaining to encoding and retrieval of words belonging to ten different semantic categories. Two popular classifiers, namely k-Nearest Neighbor and Support Vector Machine, are trained in order to predict the semantic category of the item being retrieved, based on activation patterns during encoding. The classification performance of the Functional Mesh Learning model, which range in 62-68% is superior to the classical multi-voxel pattern analysis (MVPA) methods, which range in 40-48%, for ten semantic categories.**

I. Introduction

Several methods have been developed to understand how brain processes information. One in particular, aims to predict or decode the brain state, and/or the type of information associated with cognitive processes, based on distributed patterns of activation in the brain, acquired with functional magnetic resonance imaging (fMRI) using machine learning methods [1]–[7]. One of the major motivations of this study is to propose a model for pattern analysis of fMRI data pertaining to different cognitive states using statistical learning theory. This representation involves understanding, manipulating and predicting the behaviour of the very complex nature of human brain. Massively coupled dynamic interactions of the brain at many scales cannot be fully understood by only employing the measurements recorded from the individual voxels. Therefore, there has been growing interest in using brain connectivity to reveal interactions between spatially distant regions. Brain connectivity describes neural processes as the outcomes of dynamic coordination among smaller elements [8]. Three main types of brain connectivity are reported in the literature: i) structural connectivity, basically reveals anatomic connections (pathways) of brain, such as physical links between neural elements, ii) functional connectivity, defined as statistical dependence between remote neural elements or regions across time, e.g. correlation and iii) effective connectivity, which analyses brain connectivity using causal effects between neural elements, resulting in causal activation paths [9], [10]. Connectivity for decoding is mostly used for model selection and/or defining the neighbourhood of seed neural elements or regions [11]. For instance, in a study by McIntosh *et al.*, partial least squares for activation analysis is performed to construct a cross block covariance matrix using PET data [12]. Correlation based measures such as correlation/partial correlation, Granger causality, independent component analysis (ICA), mutual-information or coherence are used for the selection of different functional interdependence functions [13]–[15]. Ryali *et al.* measure sparse-partial correlation between multiple regions using elastic net penalty, which combines L1 and L2 norm regularization terms, in order to improve the sensitivity of the correlation measure [16]. Patel *et al.* propose a conditional dependence model which accounts for an imbalance between class conditional and posterior probabilities, to achieve at a measure of connectivity [17]. Unlike correlation measures, Shier *et al.* train a classifier to decode cognitive states after constructing functional connectivity matrices, analysing increasing connectivity regions by subtracting connectivity matrices for each state [7]. Richiardi *et al.* [6] construct functional connectivity matrices by using pair-wise Pearson correlation coefficients and employ graph matching to decode brain states.

In this study, we introduce an algorithm for modelling cognitive processes, based on the functional and structural connectivity in the brain. Structural connectivity is utilized for anatomic parcellation of the brain regions by clustering the voxel intensity values measured by fMRI. Next, functional connectivity is utilized within the clusters by different correlation measures. Functional connectivity matrices are formed to define functional neighbourhood of a voxel. A local mesh is formed for each voxel (called the seed voxel) by including the functionally closest neighbours (called the surrounding voxels)

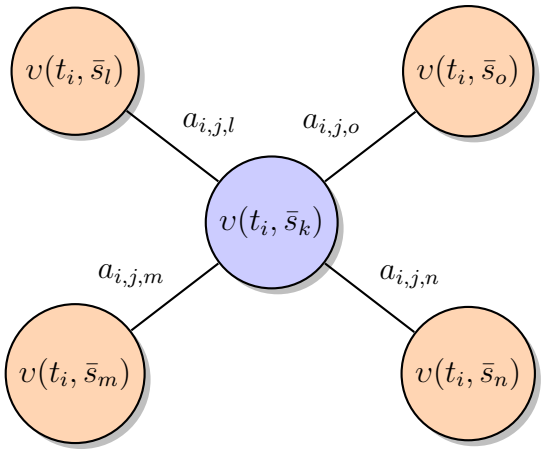

Fig. 1: Mesh diagram which represents a seed voxel $\upsilon(t_i, \bar{s}_k)$ and it's p-nearest neighbours at time instant t_i .

in the mesh. The relationships between the seed voxel and the surrounding voxels are modelled by estimating the arc weights of the mesh in a linear regression model. The arc weights, called Functional Connectivity-aware Local Relational Features (FC-LRF), represent the relationship of each voxel to its functionally closest neighbours. Finally, the proposed FC-LRF features are used to train a classifier which recognizes type of information and/or cognitive state. In the current study, we particularly focused on classification of the type of information being encoded and retrieved during memory operations. During the experiment, participants studied a list of words selected from one of ten pre-defined semantic categories and made recognition memory judgements while neural activation was recorded using fMRI [18], [19]. Accordingly, we tested whether is the proposed machine learning algorithm can successfully identify and differentiate the type of information (i.e. the semantic category that the word belongs to) which is represented in the brain at a given time considering distributed patterns of brain activity associated with and during memory encoding and retrieval.

II. Mesh Learning and Local Relational Features (LRF)

In this study, BOLD signals $\upsilon(t_i, \bar{s}_j)$ are measured at time instants $t_i, i = 1, 2, 3, \cdots, N$, at voxel coordinates $\bar{s}_j, j = 1, 2, 3, \cdots, M$, where N is the number of time samples, and M is the number of voxels. The data set $D = \{\upsilon(t_i, \bar{s}_j)\}$ consists of the voxels $\upsilon(t_i, \bar{s}_j)$, which are distributed in brain in three dimensions. Therefore, the position $\bar{s}_j = (x_j, y_j, z_j)$ of a voxel $\upsilon(t_i, \bar{s}_j)$ at time instant t_i is a three dimensional vector. At each time instant t_i, the participant is processing (either encoding or retrieving) a word belonging to a cognitive process. Therefore, the samples $\upsilon(t_i, \bar{s}_j)$ has an object label at each time instance. In Mesh Learning [20], the cognitive states are modelled by local meshes for each individual voxel, called seed voxel $\upsilon(t_i, \bar{s}_j)$, which is defined in a neighbourhood system η_p (see;Figure 1). In this mesh, voxel $\upsilon(t_i, \bar{s}_j)$ is connected to p-nearest neighbouring voxels $\{\upsilon(t_i, \bar{s}_j)\}_{k=1}^{p}$ by the arcs with weights $\{a_{i,j,k}\}_{k=1}^{p}$. Therefore, the relationship among the BOLD signals measured at each voxel, are represented by the arc weights. p-nearest neighbours, η_p, are defined as the spatially-nearest neighbours to the seed voxel, where the distances between the voxels are computed using Euclidean distances between the spatial coordinates $\bar{s}_j$ of the voxels in brain. The arc weights $a_{i,j,k}$ of the mesh are estimated by the following linear regression equation:

$$\upsilon(t_i, \bar{s}_j) = \sum_{\bar{s}_k \in \eta_p} a_{i,j,k}\ \upsilon(t_i, \bar{s}_k) + \varepsilon_{i,j}, \tag{1}$$

where $\varepsilon_{i,j}$ indicates the error of voxel $\upsilon(t_i, \bar{s}_j)$ at time instant t_i, which is minimized for estimating the arc weights $a_{i,j,k}$. This procedure is conducted by minimizing the expected square error defined as follows,

$$E(\varepsilon_{i,j}^2) = E\left(\left(\upsilon(t_i, \bar{s}_j) - \sum_{\bar{s}_k \in \eta_p} a_{i,j,k}\ \upsilon(t_i, \bar{s}_k)\right)^2\right), \tag{2}$$

where $\eta_p(\bar{s}_j)$ is the set of p-nearest neighbours of the j^{th} voxel at location $\bar{s}_j$.

Minimizing equation (2) with respect to $a_{i,j,k}$ is accomplished by employing Levinson-Durbin recursion [21], where $E(\cdot)$ is the expectation operator. The arc weights $a_{i,j,k}$, which are computed for each seed voxel at each time instant t_i, is used to form the mesh arc vector $\bar{a}_{i,j} = [a_{i,j,1}\ a_{i,j,2}\ \cdots\ a_{i,j,p}]$. Furthermore, a mesh arc matrix A_j is constructed by concatenating the mesh arc vectors at each time instant, $A_j = [\bar{a}_{1,j}\ \bar{a}_{2,j}\ \cdots\ \bar{a}_{N,j}]^T$. Finally, feature matrix $F = [A_1\ A_2\ \cdots\ A_M]$ which represents the Local Relational Features (LRF), is constructed. The feature matrix, extracted during both memory encoding and retrieval stages is further used in training and testing phases in the classification of cognitive processes, respectively. For the details of the mesh learning algorithm see [20], [22], [23].

The motivation of representing voxels in the brain by local meshes can be validated by analysing an individual voxel's intensity change and the change of the sum of squared difference of intensities $d_{\bar{s}_j, \eta_p(\bar{s}_j)} = \sum_{\bar{s}_k \in \eta_p(\bar{s}_j)} [\upsilon(t_i, \bar{s}_j) - \upsilon(t_i, \bar{s}_k)]^2$ in the neighbourhood of that voxel in time. Individual voxel intensity values, which are measured at each time instant, do not possess any discriminative information as illustrated in Figure 2 with red line. Note that the signal intensity value for a voxel is almost constant for each time instant. Since the measurements along the time axis correspond to separate cognitive processes, in most of the problems, it is unlikely to discriminate them by using standard multi-voxel pattern analysis (MVPA) methods, which classify the voxel intensity values by a machine learning tool. On the contrary, there is a slight variation of the sum of squared distances of intensity values in differing neighbour sizes. The above observation slightly shows that the relationships among voxels carry more information than individual voxel intensity values, at each time instant.

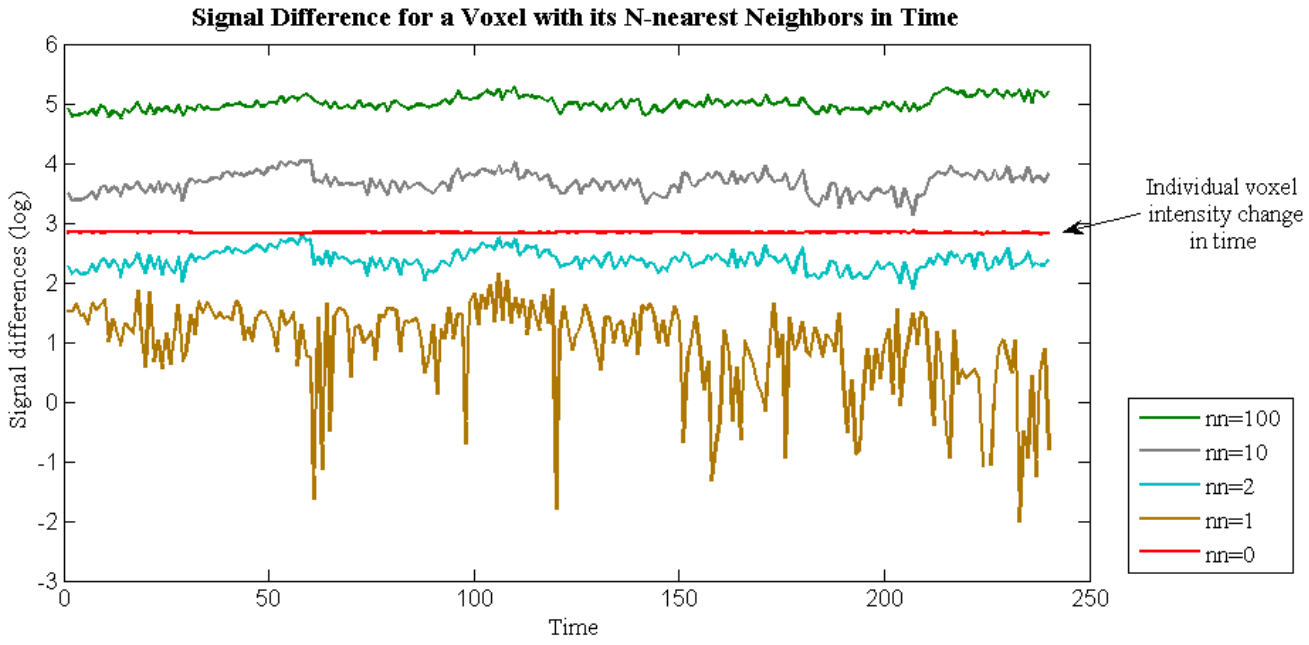

Fig. 2: Sum of squared difference, $d_{\bar{s}_j,\eta_p(\bar{s}_j)}$, of intensity values for a voxel and its N-nearest neighbouring voxels over time in log space. The time axis indicates the fMRI measurements from 10 semantic categories.

III. Functional Connectivity in the Brain

The estimated LRF vectors, which represent relationships among the voxels in the same neighbourhood system, have a high discriminative power compared to the individual voxel intensity values. As a result, the Mesh learning algorithm proposed by [20] performs better than the well-known individual voxel based algorithms (see also; Table II). However, employing the Euclidean distance to form the neighbourhood system may not fully represent the activation patterns in the brain, where the spatially distant neurons might exhibit functional connectivity. *Nearest* neighbourhood in the mesh model implies spatial surroundings of the seed voxel when Euclidean distance is used, which may not be the case during cognitive processing. Additionally, it is well known that spatially close voxels are strongly coupled during cognitive processes [24]. Therefore, using Euclidean distance for defining neighbourhoods for voxels may cause redundant meshes and mesh arc weights in a feature matrix. A partial improvement for this problem can be accomplished by the usage of functional connectivity. Selecting functional neighbours for each voxel and constructing the meshes based on the functional neighbourhood results in a more discriminative feature matrix improving the classification performance.

A. Functional Connectivity

Given the time series of voxels $\upsilon(\mathbf{t}, \bar{s}_i)$ and $\upsilon(\mathbf{t}, \bar{s}_j)$, where $\mathbf{t} = (t_1, t_2, \cdots, t_N)$ is the time vector as the variables are consecutive time instants, functional connectivity is defined as the measure of "similarity" between time series of these voxels. The voxels are considered to be functionally connected if they have "similar" functional properties. Therefore, the functional connectivity depends on the similarity measure. The "similarity" can be measured, for example, by estimating the correlation or covariance between pairs of time series. Functional connectivity is expected to capture patterns of deviations between distributed and often spatially remote regions in brain [25] and constructed using an inter-regional analysis.

B. Functional Connectivity Graph

In order to represent functional connectivity in brain, we define a graph $G = (V, E)$, where $V = \{\vartheta_j\}_{j=1}^{M}$ is the set of nodes (vertices) and $E = \{e_{jk}\}_{j,k=1}^{M}$ is the set of edges. In this representation, a node ϑ_j corresponds to a time series, $\upsilon(\mathbf{t}, \bar{s}_j)$, which is measured at an individual voxel and an edge between ϑ_j and ϑ_k, is represented as $e_{jk} = \rho_{jk}$, where ρ_{jk}, is the functional connectivity coefficient, which is computed using a functional similarity measure between time series of voxel signals $\upsilon(\mathbf{t}, \bar{s}_j)$, $j = 1, 2, 3, \cdots, M$, using equation (3).

In this study, edges in the functional connectivity graph are represented by symmetric dependence measures, in the time domain. It has been suggested that correlation based measures are well suited for functional connectivity analysis [26]. Consequently, we use zero-order correlation (cross-correlation) to measure the functional similarity between time-series. The

zero-order correlation coefficient between two nodes, voxels ϑ_j and ϑ_k in our case, ρ_{jk}, is given by

$$\rho_{jk} = \frac{cov_{jk}\big(\upsilon(\mathbf{t}, \bar{s}_j),\ \upsilon(\mathbf{t}, \bar{s}_k)\big)}{\sqrt{var_j\big(\upsilon(\mathbf{t}, \bar{s}_j)\big) \cdot var_k\big(\upsilon(\mathbf{t}, \bar{s}_k)\big)}}, \tag{3}$$

where cov_{jk} is the covariance of the signals measured at two voxels, and var_j is the variance of the signals measured at a voxel $\upsilon(\mathbf{t}, \bar{s}_j)$ and $\rho_{jk} \in [-1, 1]$.

C. Local Patches

Constructing a functional connectivity graph by considering all voxels as individual nodes introduces scalability problems. In order to reduce the computational complexity, the voxels are first clustered with respect to their locations, where each cluster is called a local patch. Then, the functional connectivity graph is formed for the voxels in each local patch with approximately size π. This approach reduces the computational complexity from $O(M^2)$ to $O(C\pi^2)$ where M is the number of voxels, C is the number of local patches. Note that $\pi \ll M$, in practice.

The local patches are constructed by clustering the whole dataset $D = \{\upsilon(t_i, \bar{s}_j)\}$, $i = 1, 2, 3, \cdots, N$, $j = 1, 2, 3, \cdots, M$, using Euclidean distance among spatial locations of voxels $\bar{s}_j = (x_j, y_j, z_j)$ in a self-tuning spectral clustering algorithm [27]. After partitioning the whole dataset D into C clusters, functional connectivity is measured locally within these clusters. A cognitive process is then represented in a local patch (cluster) m, using a within cluster functional connectivity matrix FC_m, each of which forms the set of functional connectivity matrices $FC = \{FC_m\}_{m=1}^{C}$ which is employed in the model selection for mesh learning algorithm. Details of the within cluster functional connectivity matrix computation process are given in **Algorithm 1**. Figure 3, represents the local connectivity patterns in two generated clusters.

Algorithm 1 `Computation of Within-Cluster Functional Connectivity Matrices`

Input : Dataset : $D = \{\upsilon(t_i, \bar{s}_j)\}$, $i = 1, 2, \cdots, N, j = 1, 2, \cdots, M$
Number of Clusters: C

Output : The Set of Functional Connectivity Matrices ***FC***

```
FC ← ∅
[c_1, c_2, ..., c_C] ← clusterVoxelsByLocation([s̄_1, s̄_2, ..., s̄_M])
for m = 1 to C do
    for each pair (j, k) ∈ c_m do
        FC_m(j, k) ← ρ_jk      // using Equation 3
    end for
    FC ← FC ∪ FC_m
end for
return FC
```

IV. Functionally Connected Mesh

We define a local mesh around each voxel which consists of the set of functionally connected voxels. These meshes are then used to extract LRF features from the meshes which consist of functionally similar voxels. The suggested model is called Functional Mesh Learning and the extracted LRF features are called Functional Connectivity aware LRF (FC-LRF).

A. Functional Connectivity Aware Local Relational Features (FC-LRF)

Each element of functional connectivity matrix FC_m, represents a pair-wise correlation of two voxels, in a local patch. Since, the correlation between any two nodes lies in the interval $[-1, 1]$ interval, BOLD time-series of two nodes can either be positively correlated or negatively correlated.

Mathematically speaking, the functionally nearest neighbour of $\upsilon(t_i, \bar{s}_j)$ is defined as,

$$\eta_1^{fc}\big[\upsilon(t_i, \bar{s}_j)\big] = \big\{\upsilon(t_i, \bar{s}_k)\ : max(\rho_{jk}), \quad \forall \upsilon(t_i, \bar{s}_j) \in FC_m(j', \cdot)\ \big\}, \tag{4}$$

Then, the p-functional neighbourhood of a voxel $\upsilon(t_i, \bar{s}_j)$ is generated from the $(p-1)$-functional neighbourhood iteratively, selecting the functionally nearest neighbour of that voxel from $\eta_{p-1}^{fc}\big[\upsilon(t_i, \bar{s}_j)\big]^c$, where c indicates the complement set of η_{p-1}^{fc}. p-functionally nearest neighbours of voxel $\upsilon(t_i, \bar{s}_j)$ are obtained by adding the voxels in $\eta_{p-1}^{fc}\big[\upsilon(t_i, \bar{s}_j)\big]$ to the functionally nearest neighbour of η_p^{fc}, as follows;

$$\eta_p^{fc}\big[\upsilon(t_i, \bar{s}_j)\big] = \big\{\upsilon(t_i, \bar{s}_k)\ \cup\ \eta_{p-1}^{fc}\big[\upsilon(t_i, \bar{s}_j)\big] : max(\rho_{jk}), \quad \upsilon(t_i, \bar{s}_j) \in \eta_{p-1}^{fc}\big[\upsilon(t_i, \bar{s}_j)\big]^c\ \big\}, \tag{5}$$

For a voxel ϑ_j at location $\bar{s}_j$, the set of p-functionally nearest neighbors η_p^{fc}, consists of the p of the most strongly correlated voxels in row j of the functional connectivity matrix $FC_m(j', \cdot)$, which is computed in **Algorithm 1**, where m is the index of the cluster which voxel $\upsilon(t_i, \bar{s}_j)$ belongs to and j' is the translated index of the voxel in FC_m.

Equation (5) employs only positively correlated samples (ρ_{jk} values close to $+1$). Another definition for functional neighbourhood can be given by using the negatively correlated samples (ρ_{jk} values close to -1). In this case, $max(\cdot)$ operation of equation (5) is replaced by $min(\cdot)$ operation. In Figure 3, functionally nearest neighbour selection is illustrated by using most positively correlated (obtained by $max(\cdot)$ operation) and most negatively correlated voxels (obtained by $min(\cdot)$ operation). Note that, the order of FC-LRF cannot exceed the minimum number of voxels in all clusters, $p \leqslant \pi_m\ \forall m = 1, 2, 3, \cdots, C$. Details of the FC-LRF extraction are given in **Algorithm 2**.

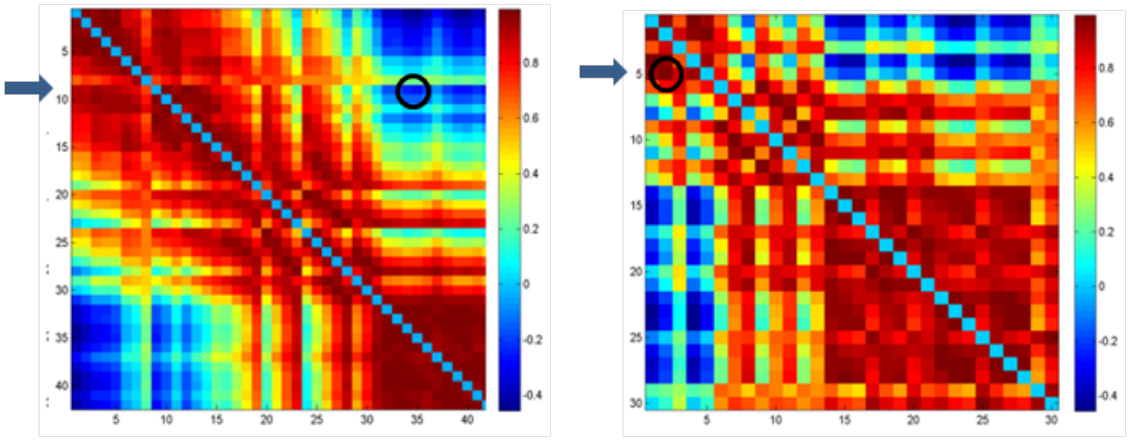

(a) (b)

Fig. 3: Sample functional connectivity matrices constructed for local patch 104 (3a) and 54 (3b) used in experiments. Each row of represents the correlation between a seed node (row index) and all other nodes in the local patch. The most positively correlated neighbor for voxel 5 in cluster 104 is voxel 2 and indicated with a circle (3b), the most negatively correlated neighbor for voxel 9 in cluster 54 is voxel 35 and indicated with a circle (3a).

Algorithm 2 `Extract Functional Connectivity Aware Local Relational Features (FC-LRF)`

Input : Dataset : $D = \{v(t_i, \bar{s_j})\}$,
Order of FC-LRF: p
Functional Connectivity Matrices: ***FC***

Output : Feature matrix F

1: **for** $j = 1$ **to** M **do**
2: Compute $p-functional-neighborhood\ \eta_p^{fc}\left[v(\cdot, \bar{s}_j)\right]$ of $v(\cdot, \bar{s}_j)$ by analysing ***FC***
3: **for** $i = 1$ **to** N **do**
4: Compute $\bar{a}_{i,j}$ by minimizing (2) **if** $\eta_p^{fc}\left[v(\cdot, \bar{s}_j)\right] \neq \emptyset$
5: **end for**
6: Construct A_j using $\bar{a}_{i,j}$
7: **end for**
8: Construct F using A_j
9: **return** F

V. Experiments for the fMRI Data Collection

In the experiment, a participant is shown lists of words selected from a pre-defined semantic category, while being scanned using fMRI, see [18], [19]. After the presentation of each study list, the participant solves math problems and following this delay period, decides whether a probe word matches one of the members of the study list ("old" or "new"). Employing a delay period (about 14 sec during which the participant solved math problems) allows independent assessment of encoding related (i.e. study list period) brain activation from retrieval related (i.e. during the test probe) activity patterns. With this approach, one can test whether it is possible to identify and differentiate semantic categories of information that is represented in the brain at a given time based on distributed patterns of brain activity associated with and during cognitive processing. A total of ten semantic categories were used in the study, which are *animals*, *colors*, *furniture*, *body parts*, *fruits*, *herbs*, *clothes*, *chemical elements*, *vegetables* and *tools*. We used the neural activation patterns collected during encoding and retrieval phases, to train and test the classifier to predict the semantic categories.

The neuroimaging data underwent standard preprocessing stages before the pattern analysis step. Image processing and data analysis were performed using SPM5 (http://www.fil.ion.ucl.ac.uk/spm/). Following quality assurance procedures to assess outliers or artefacts in volume and slice-to-slice variance in the global signal, functional images were corrected for differences in slice acquisition timing by re-sampling all slices in time to match the first slice, followed by motion correction across all runs (using sinc interpolation). Functional data were then normalized based on MNI stereotaxic space using a 12-parameter affine transformation along with a non-linear transformation using cosine basis functions. Images were re-sampled into 2-mm cubic voxels and then spatially smoothed with an 8-mm FWHM isotropic Gaussian kernel. Next, the functional data were detrended to account for baseline shifts across runs and for scanner drift across the entire session for the pattern analysis. Consistent with previous research of Polyn *et al.*, onsets were shifted forward by three points to account for the hemodynamic response lag [28].

VI. Implementation of the Functional Mesh Learning Algorithm

Our dataset consists of 240 training samples from encoding phase and 239 test samples from the retrieval phase with 24 samples in each of 10 semantic categories. Our region of interest consisted of 8142 voxels covering the lateral temporal cortex. Results for FC-LRF were generated using k-nearest neighbor (k-nn) and Support Vector Machine (SVM) methods. The k value of k-nn and kernel parameters of SVM classifier are selected using cross validation in training set. The number

TABLE I: Performance results of the Functional Mesh Learning algorithm. Performance measures are indicated Recall as R, Precision as P and F-Score as F on the header row.

	K-nn						SVM					
Class Label	Positively Correlated Neighbors			Negatively Correlated Neighbors			Positively Correlated Neighbors			Negatively Correlated Neighbors		
	P	R	F	P	R	F	P	R	F	P	R	F
1	63	58	60	63	54	58	54	54	54	57	54	55
2	79	75	77	**75**	75	75	61	71	65	63	**79**	**70**
3	**79**	**76**	**78**	75	71	73	**76**	**79**	**78**	69	75	72
4	74	68	71	78	61	68	64	75	69	58	61	60
5	58	68	63	58	59	59	58	46	51	55	50	52
6	63	72	67	63	**81**	71	75	63	68	**81**	54	65
7	67	75	71	**75**	71	73	62	67	64	65	71	68
8	71	64	67	63	61	62	67	58	62	68	54	60
9	67	56	61	67	65	66	55	67	60	57	71	63
10	54	65	59	67	73	70	52	50	51	63	50	56
Avg	67	68	68	68	67	68	62	63	63	64	62	63

of clusters C in the proposed algorithm is a user specified parameter. Since the number of voxels in all clusters π_m is always much higher than FC-LRF order p, regardless of the cluster size, similar functionally connected meshes are formed. Therefore, it has practically no effect on the performance of the algorithm. This fact is illustrated in the performance results in Table III. Graph theoretic approaches can be employed after calculating functional connectivity matrices in order to partition connectivity matrices such as [29], [30], but this will introduce additional thresholds and user specified parameters, thus spared as a future work. Three different correlation variants are employed to capture functional similarity between nodes; i) cross-correlation which is given in equation 3, ii) peak correlation which captures the relationships between activation peaks and iii) scan correlation, which measures the correlations of waveforms at a specific scan of interest. The overall performance of the algorithm is improved only by 2-4% percent by employing improved correlation measures as peak correlation and scan correlation. In addition, we employ two different functionally-nearest neighbour selection approaches namely, selecting positively and negatively correlated neighbours. The performance results are illustrated in Table I. Functional Connectivity Toolbox implementation [31] is used for the computation of the correlation measures.

TABLE II: Classification Performance Comparison of Proposed Algorithm.

Method Empoyed	**Accuracy**	
	K-nn	**SVM**
Classical MVPA method (Without LRF)	48	40
Mesh Learning [16]	58	45
Functional Mesh Learning using Positive Correlation	68	63
Functional Mesh Learning using Negative Correlation	67	62

The results in Table II show that the employment of functional connectivity in the mesh learning algorithm [20] improves classification performances, considerably. When we classify the raw features of 8142 voxels (without LRF), we observe 48% and 40% performances. Note that Mesh Learning increases the performances to 58% and 45% and Functional Mesh Learning further increases the performances up to 68% and 63% using k-NN and SVM methods, respectively. The main issue which increases the performance is basically the selection of nearest neighbours by using functional connectivity of the voxels in brain.

TABLE III: Classification Performances for Varying Number of Local Patches using zero order correlation.

Number of Local Patches	**32**	**64**	**128**	**256**	**Std.Dev.**
Recall	66,97	66,56	67,81	67,39	0,54
Precision	68,44	67,71	67,84	67,77	0,33

VII. Conclusion

In this study, we propose a new machine learning approach, Functional Mesh Learning, in order to classify cognitive process, based on distributed patterns of neural activation patterns in the brain. In the current data set, the model was tested during memory process and performed successfully. The proposed method employs functional connectivity in order to define local meshes to represent the relationships between the voxels and their p-functionally nearest neighbours. Our goal is to be able to model cognitive processes based on neural activation patterns in the brain. The present set of results indicate that the suggested Functional Mesh Learning model can be used to classify cognitive states and types of information represented during these cognitive operations based on distributed patterns of brain activity. In the current study, we only focused on modelling memory encoding and retrieval processes. Future research extending these findings to a wider range of cognitive operations would bring additional insight into the generality of the proposed algorithm. We expect further improvement by incorporating additional domain knowledge (i.e. anatomical maps, DTI) to the learning model and eliminating drawbacks such as the linearity of the mesh model, selecting the optimal FC-LRF order value p, lack of modelling brain hierarchy.

REFERENCES

[1] X. Wang, R. Hutchinson, and T. M. Mitchell, "Training fMRI Classifiers to Detect Cognitive States across Multiple Human Subjects," *IN NIPS03*, vol. 16, 2003.

[2] K. A. Norman, S. M. Polyn, G. J. Detre, and J. V. Haxby, "Beyond mind-reading: multi-voxel pattern analysis of fMRI data." *Trends in cognitive sciences*, vol. 10, no. 9, pp. 424–30, Sep. 2006.

[3] J.-D. Haynes and G. Rees, "Decoding mental states from brain activity in humans." *Nature reviews. Neuroscience*, vol. 7, no. 7, pp. 523–34, Jul. 2006.

[4] A. Battle, G. Chechik, and D. Koller, "Temporal and cross-subject probabilistic models for fmri prediction tasks," in *NIPS'06*, 2006, pp. 121–128.

[5] C.-J. Lin and M.-H. Hsieh, "Classification of mental task from EEG data using neural networks based on particle swarm optimization," *Neurocomputing*, vol. 72, no. 4-6, pp. 1121–1130, Jan. 2009.

[6] J. Richiardi, H. Eryilmaz, S. Schwartz, P. Vuilleumier, and D. Van De Ville, "Decoding brain states from fMRI connectivity graphs." *NeuroImage*, vol. 56, no. 2, pp. 616–26, May 2011.

[7] W. R. Shirer, S. Ryali, E. Rykhlevskaia, V. Menon, and M. D. Greicius, "Decoding subject-driven cognitive states with whole-brain connectivity patterns." *Cerebral cortex (New York, N.Y. : 1991)*, vol. 22, no. 1, pp. 158–65, Jan. 2012.

[8] E. Bullmore and O. Sporns, "Complex brain networks: graph theoretical analysis of structural and functional systems." *Nature reviews. Neuroscience*, vol. 10, no. 3, pp. 186–98, Mar. 2009.

[9] S. L. Bressler and V. Menon, "Large-scale brain networks in cognition: emerging methods and principles." *Trends in cognitive sciences*, vol. 14, no. 6, pp. 277–90, Jun. 2010.

[10] K. J. Friston and K. J. Friston, "Functional and Effective Connectivity in Neuroimaging: A Synthesis," 1994.

[11] K. Li, L. Guo, J. Nie, G. Li, and T. Liu, "Review of methods for functional brain connectivity detection using fMRI." *Computerized medical imaging and graphics : the official journal of the Computerized Medical Imaging Society*, vol. 33, no. 2, pp. 131–9, Mar. 2009.

[12] A. McIntosh, L. Nyberg, F. Bookstein, and E. Tulving, "Differential functional connectivity of prefrontal and medial temporal cortices during episodic," *Human Brain Mapping*, 1997.

[13] H. Chen and D. Yao, "A composite ICA algorithm and the application in localization of brain activities," *Neurocomputing*, vol. 56, pp. 429–434, Jan. 2004.

[14] J. Anemüller, J.-R. Duann, T. J. Sejnowski, and S. Makeig, "Spatio-temporal dynamics in fMRI recordings revealed with complex independent component analysis." *Neurocomputing*, vol. 69, no. 13-15, pp. 1502–1512, Aug. 2006.

[15] S. Hu and H. Liang, "Causality analysis of neural connectivity: New tool and limitations of spectral Granger causality," *Neurocomputing*, vol. 76, no. 1, pp. 44–47, Jan. 2012.

[16] S. Ryali, T. Chen, K. Supekar, and V. Menon, "Estimation of functional connectivity in fMRI data using stability selection-based sparse partial correlation with elastic net penalty." *NeuroImage*, vol. 59, no. 4, pp. 3852–61, Feb. 2012.

[17] R. S. Patel, F. D. Bowman, and J. K. Rilling, "A Bayesian approach to determining connectivity of the human brain." *Human brain mapping*, vol. 27, no. 3, pp. 267–76, Mar. 2006.

[18] I. Oztekin, C. E. Curtis, and B. McElree, "The medial temporal lobe and the left inferior prefrontal cortex jointly support interference resolution in verbal working memory." *Journal of cognitive neuroscience*, vol. 21, no. 10, pp. 1967–79, Oct. 2009.

[19] I. Oztekin and D. Badre, "Distributed Patterns of Brain Activity that Lead to Forgetting." *Frontiers in human neuroscience*, vol. 5, p. 86, Jan. 2011.

[20] M. Özay, I. Öztekin, U. Öztekin, and F. T. Y. Vural, "Mesh Learning for Classifying Cognitive Processes," *Arxiv:1205.2382*, May 2012.

[21] P. P. Vaidyanathan, "The Theory of Linear Prediction," *Synthesis Lectures on Signal Processing*, vol. 2, no. 1, pp. 1–184, Jan. 2007.

[22] M. Özay, l. Öztekin, U. Öztekin, and F. T. Yarman Vural, "Neuroinformatics 2011: Modeling cognitive states using machine learning techniques," 2011.

[23] O. Fırat, M. Özay, I. Önal, l. Öztekin, and F. T. Yarman Vural, "A Mesh Learning Approach for Brain Data Modeling," in *IEEE 20th Conference on Signal Processing and Communications Applications (SIU)*, 2012.

[24] O. Sporns, "The human connectome: a complex network." *Annals of the New York Academy of Sciences*, vol. 1224, pp. 109–25, Apr. 2011.

[25] O. Sporns, "Networks of the Brain," *The MIT Press* Nov. 2010.

[26] S. M. Smith, K. L. Miller, G. Salimi-Khorshidi, M. Webster, C. F. Beckmann, T. E. Nichols, J. D. Ramsey, and M. W. Woolrich, "Network modelling methods for FMRI." *NeuroImage*, vol. 54, no. 2, pp. 875–91, Jan. 2011.

[27] L. Zelnik-manor and P. Perona, "Self-tuning spectral clustering," in *Advances in Neural Information Processing Systems 17*. MIT Press, 2004, pp. 1601–1608.

[28] S. Polyn, "Neuroimaging, behavioral, and computational investigations of memory targeting," Ph.D. dissertation, Princeton University, 2005.

[29] S. Dodel, J. Herrmann, and T. Geisel, "Functional connectivity by cross-correlation clustering," *Neurocomputing*, vol. 44-46, pp. 1065–1070, Jun. 2002.

[30] J. C. Reijneveld, S. C. Ponten, H. W. Berendse, and C. J. Stam, "The application of graph theoretical analysis to complex networks in the brain." *Clinical neurophysiology : official journal of the International Federation of Clinical Neurophysiology*, vol. 118, no. 11, pp. 2317–31, Nov. 2007.

[31] D. Zhou, W. K. Thompson, and G. Siegle, "MATLAB toolbox for functional connectivity." *NeuroImage*, vol. 47, no. 4, pp. 1590–607, Oct. 2009.